PAPER

Check for updates

Unusual redshift due to selective hydrogen bonding between F⁻ ion and sensor motif: a naked eye colorimetric sensor for F⁻ ions in an aqueous environment†

Jyotirlata Singha, Tapendu Samanta and Raja Shunmugam [iD] *

Naked-eye detection of anions is a challenging but useful technique. In this study, two novel colorimetric monomeric sensors based on highly selective 2,4-dinitrophenylhydrazine were designed, synthesized, and employed as a selective ratiometric optical sensor for F⁻ ion detection *via* the naked eye. The anion recognition properties were investigated *via* a pattern of color change as well as changes in absorbance signaling maxima. Sensor molecules were characterized by ^{1}H NMR, ^{13}CNMR, HRMS, and FTIR spectroscopy. Selectivity towards F⁻ ions was attributed to the capability of H-bonding interaction of N–H bonds, which was determined by ^{1}H NMR titration, ^{19}F NMR titration, and UV-vis spectroscopic titration. The association constants of 0.263×10^6 M⁻¹ (compound **4**) and 6.4988×10^6 M⁻¹ were calculated using the Benesi–Hildebrand equation from UV-vis spectroscopic analysis. The limit of detection (LOD) for both monomeric sensors was 68.182 nM (compound **4**) and 72.341 nM (compound **9**) and for the polymeric sensor, it was 18.98157 nM (compound **11**). Job's plot analysis revealed the existence of 1:1 complex formation of F⁻ ions with both monomeric sensor molecules. The same colorimetric response and selectivity properties were exhibited by the norbornene-based homopolymer of the polymeric sensor molecule towards F⁻ ions.

1. Introduction

All anions play an important role in both biological and environmental systems.[1,2] Among them, F⁻ ions are vital to humans because their deficiency leads to osteoporosis, and their overexposure causes weak bones and dental issues.[3–5] Hence, F⁻ ion detection and removal are important challenges nowadays. Some of the existing techniques for F⁻ ion determination include using a smartphone, an ion-selective electrode or a membrane-selective electrode, solid-state combination, optical methods, *etc.* In most of the cases, instruments are expensive and difficult to handle.[6] Therefore, developing comparatively cheaper and easy-to-handle F⁻ ion techniques is currently an attractive topic for researchers in different fields. Inorganic fluoride is mainly obtained from F⁻ ion-containing rocks, *e.g.*, apatite, fluorite, biotite, and hornblende. Other sources include volcanic ash, agricultural fertilizers, combustion of coal, *etc.* Improper disposal of fly ash on the ground surface contributes fluoride to groundwater.[7,8] The WHO-permitted range

of F⁻ ion concentration in groundwater is 0.6 mg mL⁻¹ to 1.5 mg mL⁻¹. The presence of this anionic species beyond this range is carcinogenic.[9] Hence, the superior detection and quantification of F⁻ ions is a new challenge for researchers. Among all the existing detection techniques of F⁻ ions, colorimetric detection using a simple chemical sensor has recently gained research interest due to its low cost, easy handling, and easily available environment-friendly chemical characteristics for making such a kind of sensors.[10–13] Using the colorimetric technique, we can detect anions through the naked eye, which is otherwise impossible in the case of other fluorometric probes. It also facilitates the easy detection of F⁻ ions in real water samples. So, colorimetric naked-eye recognition is an essential tool for F⁻ ion detection at the ppm-level.[14] All monomeric colorimetric sensors contain one chromogenic site and one binding site. Upon binding the analyte to the binding site of the sensor molecule, the chromogenic unit responds by changing its color, which can be seen by the naked eye. The analyte can bind to the sensor through both covalent and non-covalent ways. Non-covalent interaction is mostly electrostatic interaction, including π interaction and H-bonding interaction.[15–17] For H-bonding interaction, various research groups reported various moieties such as hydrazine-based indoles, bodipy-indole conjugates, calixpyrroles, polyamines,

Polymer Research Center, Department of Chemical Science, Indian Institute of Science Education and Research Kolkata, Mohanpur, India.
E-mail: sraja@iiserkol.ac.in
† Electronic supplementary information (ESI) available. See DOI: 10.1039/d0ma00092b
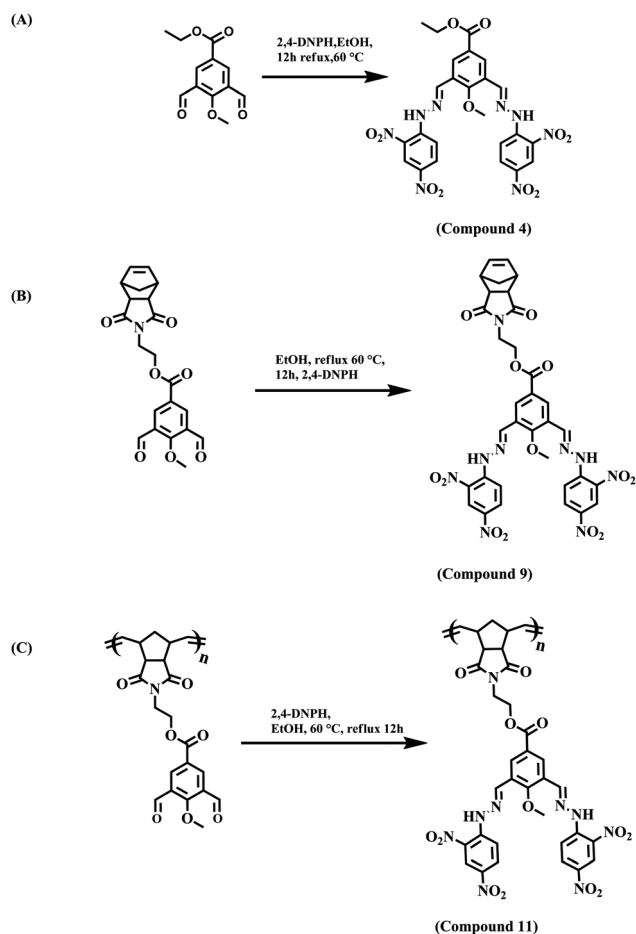
Fig. 1 Synthetic schemes of (A) compound **4**, (B) compound **9**, and (C) compound **11**.

urea, thiourea, amides, imidazole, pyrrolyl derivatives, sulpho-namides, amides, *etc.*[18–26] All the above moieties form H-bonding interactions with the smallest negatively charged dense species (mostly F$^-$ ions) and are responsible for a drastic color change.[27–34] Many of the above-mentioned systems can undergo abstraction of a proton by the classical Bronsted acid–base type of interaction at a higher concentration of F$^-$ ions.[34–42] All the above monomeric systems can detect the analyte at the ppm level through a change in the spectroscopic behavior at a particular wavelength. Among the reported F$^-$ ion sensors, very few systems have a ratiometric sensing property, which depends on various factors like concentration, electronic environment, phototransformation, *etc.* A redshift of more than 100 nm is rare for most of the existing F$^-$ ion sensors, which makes our proposed sensor very effective compared to other reported systems. In the case of a polymeric sensor, the chromogenic unit increases due to an increase in the repeating unit, so the color intensity of the polymeric sensor is higher than that of the monomeric sensor. Thus, naked-eye detection becomes easy in the case of a polymer-based sensor compared to the monomeric sensor. On the other hand, in the case of the polymeric probe, side-chain interaction between probes and analyte increases the sensing efficiency by many fold.[43]

2. Design and synthesis of sensors

To investigate the preparation of an efficient, low-cost colori-metric fluoride sensor, monomeric and polymeric sensors were synthesized as shown in Fig. 1 (all the experimental procedures are given in the ESI†). Compound **2** was prepared by incorpo-ration of the dial (Fig. S1, ESI†) to the ester of 4-hydroxybenzoic acid (compound **1** Fig. S1, ESI†) by refluxing. The condensation of the dial (compound **3** Fig. S1, ESI†) with 2,4-DNPH resulted in the final sensor molecule (compound **4** Fig. S1, ESI†). Similarly, we incorporated the dial to 4-hydroxy benzoic acid by refluxing to obtain compound **6** (Fig. S1, ESI†). For incor-poration of that dial to the norbornene monomer (compound **5** Fig. S1, ESI†), DCC coupling and column chromatography were performed, which resulted in the formation of compound **7** (Fig. S1, ESI†). Compound **9** (Fig. S1, ESI†) was isolated by the condensation of the nordial (compound **8**, Fig. S1, ESI†) with 2,4-DNPH refluxing in EtOH. Ring-opening metathesis poly-merization was performed by a Grubbs catalyst (2nd genera-tion) with molecule compound **8**, and we obtained compound **10** (Fig. S1, ESI†). The final polymeric sensor, (compound **11** Fig. S1, ESI†) was obtained through the post polymer modifica-tion reaction involving the condensation of 2,4-DNPH with compound **10** (Fig. S1, ESI†) and molecular weight was obtained by GPC (gel permeation chromatography Fig. S23, ESI†). All the above monomeric sensor molecules (compound **4** (Fig. S1, ESI†), compound **9** (Fig. S1, ESI†), and the polymeric sensor (compound **11**, Fig. S1, ESI†)) were synthesized and well-characterized using ^{1}H NMR, ^{13}CNMR, ESI-mass and FT-IR spectroscopy techniques (Fig. S2–S22, ESI†).

3. Results and discussion

3.1 Optical properties (selectivity and sensitivity study)

Absorbance spectra of the monomeric and polymeric sensors were recorded in a DMSO:H$_2$O 9:1 v/v solvent mixture with Tris–HCl buffer at pH 7.4. All three sensor molecules exhibited an absorbance maximum at λ_{max} 405 nm, and the color of the sensors was light yellow, which was visible to the naked eye (Fig. 2–4). Selectivity is an important parameter for investi-gating the performance and further applicability of a sensing mechanism. The anion receptor properties were investigated upon the addition of various interfering anions (F$^-$, Cl$^-$, Br$^-$, CH$_3$CO$_2^-$, I$^-$, ClO$_3^-$, HPO$_3^{2-}$, N$_3^-$, SO$_4^{2-}$ and NO$_3^-$), and an interesting shift in the absorbance peak was observed from 405 nm to 537 nm selectively for ion addition (Fig. 2 and 3) to the monomeric sensor compound **4** and compound **9**. The colors of the monomeric sensor solutions were changed from light yellow to dark pink instantly within seconds under the optimized conditions of Tris–HCl buffer (pH 7.4) at room temperature in a DMSO:H$_2$O 9:1 v/v solvent mixture. The above interesting selectivity was observed only for F$^-$ ions in the presence of other interfering anions for all the monomeric and polymeric sensor molecules. The F$^-$ ion is a highly electro-negative species, as a result of which a strong H-bonding interaction occurred, which is responsible for the drastic color
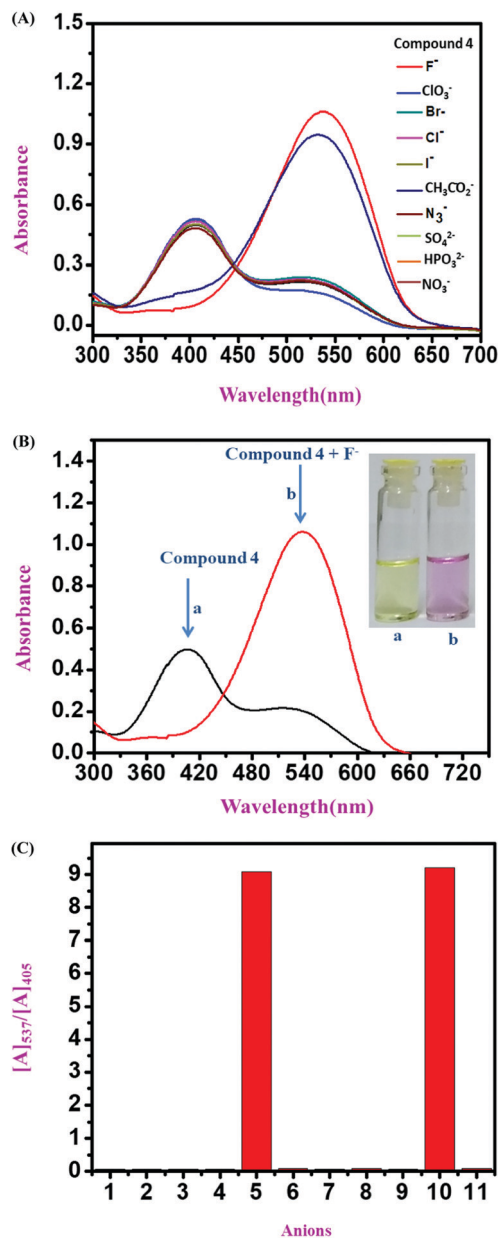
Fig. 2 (A) UV-vis absorbance spectra of compound **4** (2.5×10^{-5} M) in the presence of different anions (2.5×10^{-5} M Cl^-, Br^-, I^-, $CH_3CO_2^-$, NO_3^-, ClO_3^-, N_3^-, HPO_3^{2-}, F^-, and SO_4^{2-}) (in a $DMSO:H_2O$ 9:1 v/v solution mixture with Tris–HCl buffer at pH 7.4). (B) UV-vis absorbance spectra of compound **4** (2.5×10^{-5} M) in the absence and presence of F^- ions (2.5×10^{-5} M). (C) Corresponding bar diagram for the selectivity of compound **4** (2.5×10^{-5} M) in the presence of different anions: (1) blank, (2) Cl^-, (3) Br^- (4) I^-, (5) $CH_3CO_2^-$, (6) NO_3^-, (7) ClO_3^-, (8) N_3^-, (9) HPO_3^{2-}, (10) F^- and (11) SO_4^{2-}. (D) Pictorial presentation of compound **4** (2.5×10^{-5} M) in the presence of different anions (2.5×10^{-5} M TBA^+ salt of anions in water).

Fig. 3 (A) UV-vis absorbance spectra of compound **9** (1.5×10^{-5} M) in the presence of different anions (2.5×10^{-5} M Cl^-, Br^-, I^-, $CH_3CO_2^-$, NO_3^-, ClO_3^-, N_3^-, HPO_3^{2-}, F^-, and SO_4^{2-}) (in a $DMSO:H_2O$ 9:1 v/v solution mixture with Tris–HCl buffer at pH 7.4). (B) UV-vis absorbance spectra of compound **9** (1.5×10^{-5} M) in the absence and presence of F^- ions (2.5×10^{-5} M). (C) Corresponding bar diagram for the selectivity of compound **9** (2.5×10^{-5} M) in the presence of different anions: (1) blank, (2) Cl^-, (3) Br^- (4) F^-, (5) I^-, (6) NO_3^-, (7) $CH_3CO_2^-$, (8) N_3^-, (9) HPO_3^{2-}, and (10) SO_4^{2-}. (D) Pictorial presentation of compound **9** (1.5×10^{-5} M) in the presence of different anions (2.5×10^{-5} M TBA^+ salt of anions in water).
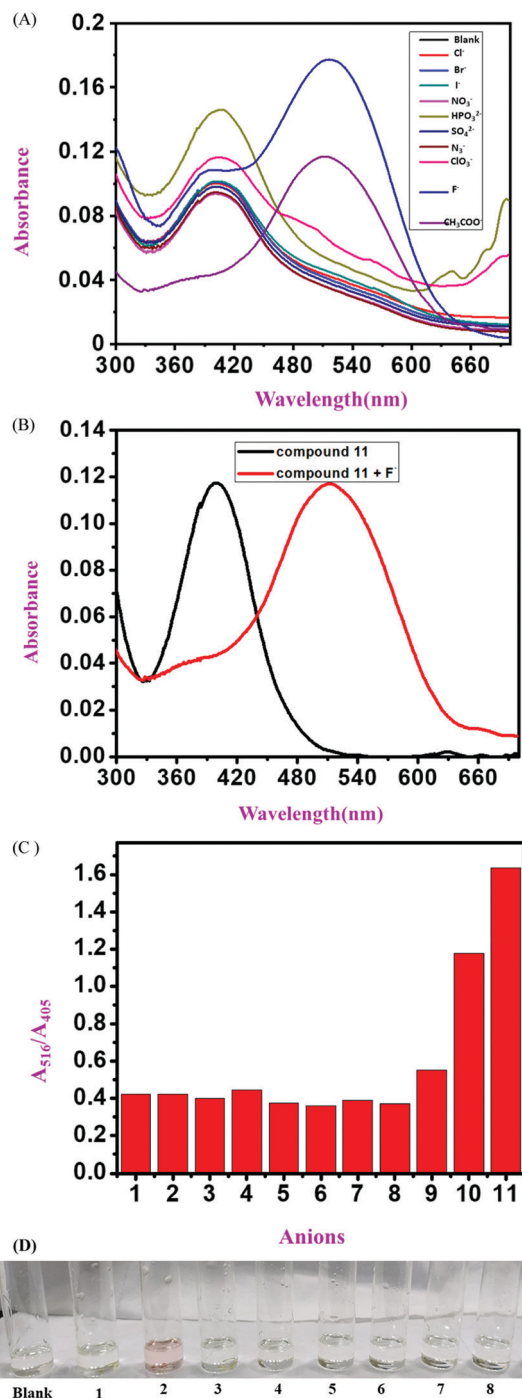
Fig. 4 (A) UV-vis absorbance spectra of compound 11 (1 mg in 2 mL of DMSO solvent) in the presence of different anions (2.5 × 10⁻⁵ M Cl⁻, Br⁻, I⁻, $CH_3CO_2^-$, NO_3^-, ClO_3^-, N_3^-, HPO_3^{2-}, F⁻, and SO_4^{2-}) (in a $DMSO:H_2O$ 9:1, v/v solution mixture with Tris–HCl buffer at pH 7.4). (B) UV-vis absorbance spectra of compound 11 (1 mg in 2 mL of DMSO solvent) in the absence and presence of F⁻ ions (2.5 × 10⁻⁵ M). (C) Corresponding bar diagram for the selectivity of compound 11 (1 mg in 2 mL of DMSO solvent) in the presence of different anions: (1) blank, (2) Cl⁻, (3) Br⁻, (4) I⁻, (5) SO_4^{2-}, (6) NO_3^-, (7) ClO_3^-, (8) N_3^-, (9) HPO_3^{2-}, (10) $CH_3CO_2^-$, and (11) F⁻. (D) Pictorial presentation of compound 11 (1 mg in 2 mL of DMSO solvent) in the presence of different anions (2.5 × 10⁻⁵ M TBA⁺ salt of anions in water).

changes of the sensors in addition to the F⁻ ion acceptor site[44,45] (Fig. 2–4).

A comparative UV-vis study was carried out in the presence of various interfering anions, F⁻, Cl⁻, Br⁻, $CH_3CO_2^-$, I⁻, ClO_3^-, HPO_3^{2-}, N_3^- NO_3^- and SO_4^{2-}, with compound 11 (polymeric sensor). The color change upon the addition of F⁻ ions for the polymeric sensor was investigated, taking 1 mg of the polymeric sensor and dissolving 1800 mL of DMSO solution. Upon the addition of F⁻ ions selectively, the absorbance maximum shifted from λ_{max} 405 nm to λ_{max} 516 nm in the 9:1 (v/v) $DMSO:H_2O$ solution mixture at pH 7.4 in the Tris–HCl buffer solution. The color of the blank polymeric sensor was light yellow, as detected by the naked eye, which changes instantly to dark pink by the addition of F⁻ ions (TBA⁺ salt 10⁻² M stock solution in water). The color intensity of the polymeric sensor was higher than that observed for the monomeric sensors because of the greater number of repeating units in the polymeric backbone than in the monomeric sensors. It was observed that, due to the polymeric repeating unit, the spectra were broad for both blank polymeric sensors and in the presence of TBAF. The more intense and drastic naked eye and spectroscopic color changes are one of the advantages of polymeric sensors compared to the monomeric sensors with the selective addition of F⁻ ions (Fig. 4).

3.2 Spectroscopic titration study

3.2.1 UV-vis spectroscopic titration. To investigate the interaction mechanism between fluoride and sensor molecules, concentration-dependent UV-vis titration studies were carried out with (2.5 × 10⁻⁶ M) compound 4 and 10⁻⁴ M F⁻ ions as a stock solution in the $DMSO:H_2O$ (9:1 v/v) solution in the presence of Tris–HCl buffer solution (pH 7.4) (Fig. 5). With the gradual addition of F⁻ ions into the sensor (compound 4) solution, the absorbance at λ_{max} 405 nm for the monomeric sensors decreased, and a new absorbance band gradually increased at λ_{max} 537 nm. Upon the addition of 2.5 × 10⁻⁶ M F⁻ ions (4 equivalent F⁻ ion), a saturation point was attained by the monomeric sensor (for compound 4). For the concentration-dependent titration experiment, compound 9 was taken as a 2.5 × 10⁻⁶ M solution in DMSO solvent with 10⁻³ M F⁻ ions as a stock solution (TBA⁺ salt). Unlike compound 4, in the case of compound 9, the absorption maximum at λ_{max} 405 nm also gradually decreased upon the addition of the F⁻ ion solution, and a new maximum was generated at λ_{max} 537 nm in the medium. A saturation point was achieved at 3.0 × 10⁻⁵ M F⁻ ion concentration. A polymeric sensor molecule (1 mg/2 mL DMSO solvent) was obtained upon the addition of F⁻ ions (10⁻³ M). A saturation point was achieved in the (6.5 × 10⁻⁵ M) F⁻ ion solution. The absorbance maximum at λ_{max} 405 nm decreased, and a new absorption maximum was generated at λ_{max} 516 nm. A saturation point was achieved in the (6.5 × 10⁻⁵ M) F⁻ ion solution. Due to the high redshift of absorption spectra from λ_{max} 405 nm to λ_{max} 537 nm (for the monomeric sensor), and from λ_{max} 405 nm to λ_{max} 516 nm (for the polymeric sensor), an isosbestic point was observed at about λ_{max} 444 nm (for all sensor molecules), which provides
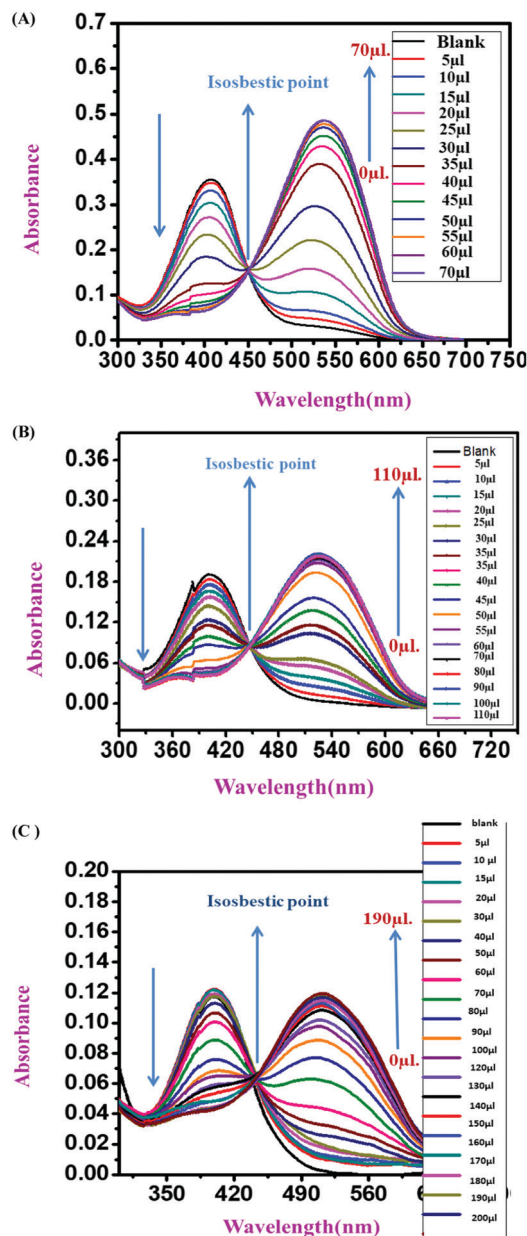
Fig. 5 UV-vis titration spectra for (A) compound **4** (2.5×10^{-6} M); (B) compound **9** (1.5×10^{-5} M); (C) compound **11** (1 mg in 2 mL of DMSO : H$_2$O [9 : 1 v/v] solvent) in the presence the TBA$^+$ salt of F$^-$ ions (10^{-4} M stock solution, 10^{-3} M and 10^{-3} M stock solution) in the DMSO : H$_2$O (9 : 1 v/v) solution with Tris–HCl buffer (pH 7.4).

the strongest evidence for the interaction of the sensor with the analyte. So, from the concentration-dependent UV-vis titration spectra, it was observed that the analyte was interacting with the monomeric and polymeric sensors in a ratiometric fashion. During the experiment, when the F$^-$ ion concentration was increased gradually, the color of the monomeric sensor changed from light yellow to dark pink in the cuvette, as detected by the naked eye.[36,37] A_{537}/A_{405} (for monomeric sensors) and A_{516}/A_{405} (for the polymeric sensor) were linearly and positively correlated with the F$^-$ ion concentration, as shown in Fig. 5.

As the sensors contain a strong electron-withdrawing –NO$_2$ group, it withdraws electrons from the NH group, resulting in a partially positive charge on the H-atom. This positively charged H atom is a harder acid in nature. The F$^-$ ion is a hard base due to its high negative charge density and smaller size than the other interfering anions (F$^-$, Cl$^-$, Br$^-$, CH$_3$CO$_2^-$, I$^-$, ClO$_3^-$, HPO$_3^{2-}$, N$_3^-$, SO$_4^{2-}$ and NO$_3^-$). As a result of the HSAB principle, the F$^-$ ion can make a strong H-bonding interaction with partially positively charged H-atoms of NH groups present in both the monomeric and polymeric sensors.[36] Because of this reason, the sensor molecules undergo interaction ratiometrically with F$^-$ ions.

3.2.2 ^{1}H NMR titration study. For the further investigation of the interaction mechanism, 5 μL of F$^-$ ions (10^{-2} M) was added to the monomeric sensors of concentration 10^{-3} M in the 0.5 M DMSO-d$_6$ solvent, followed by NMR titration. The NMR spectra showed that, after the addition of TBAF, the NH peak at around 12 ppm vanished, and a triplet was formed at around 16 ppm. Besides, the splitting number of the aromatic peaks was found to decrease compared to the splitting before the addition of the analyte to the monomeric sensors. A new peak was generated at about 16 ppm, which implies the formation of HF$_2^-$. This observation indicates that the F$^-$ ion abstracted the H-atom from the NH group, making all the sensor molecules negatively charged. This abstraction of a H-atom generated a highly water-soluble species, HF$_2^-$, in the medium. The negative charge formed due to the abstraction of H-atoms can delocalize from the N atoms all over the molecule, resulting in a decreased splitting of all aromatic peaks due to ICT.[37] Here, a naked-eye color change was observed from light yellow to dark pink in the NMR tube itself upon the addition of F$^-$ ions to the sensors due to strong ICT (intermolecular charge transfer) during the titration experiment (Fig. 6).

3.2.3 ^{19}F NMR titration study. To investigate the interaction of F$^-$ ions with the monomeric sensors (compound **4** and compound **9**), a ^{19}F NMR titration experiment was performed using a Bruker 500 MHz instrument. Then, by fixing the concentration of monomeric sensors (10^{-2} M for both), solutions with the TBAF concentration of 1 M (stock solution concentration) (for compound **4**) and TBAF concentration of 10^{-1} M (stock solution concentration) were added in 5 μL amounts, and spectra were recorded after every addition of F$^-$ ions. Then, all ^{19}F NMR spectral data were plotted (Fig. 7), and it was observed that, for compound **4**, the addition of F$^-$ ions first abstracted the H from NH to produce HF$_2^-$, which gives a ^{19}F NMR peak at -150 ppm. A further increase in the concentration of F$^-$ ions resulted in one more peak at -110 ppm, which was due to the interaction of F$^-$ ions with sensor molecules.[37] From the above experiment, we can conclude that with the increasing concentration of F$^-$ ions, two different electronic-environmental fluorides existed, one is HF$_2^-$ and the other one is due to sensor-bound fluoride species. For another sensor, i.e., compound **9**, a similar experiment was performed; the 10^{-2} M concentration of the sensor compound was fixed, and a 10^{-1} M F$^-$ ion solution was added to it gradually. The ^{19}F NMR
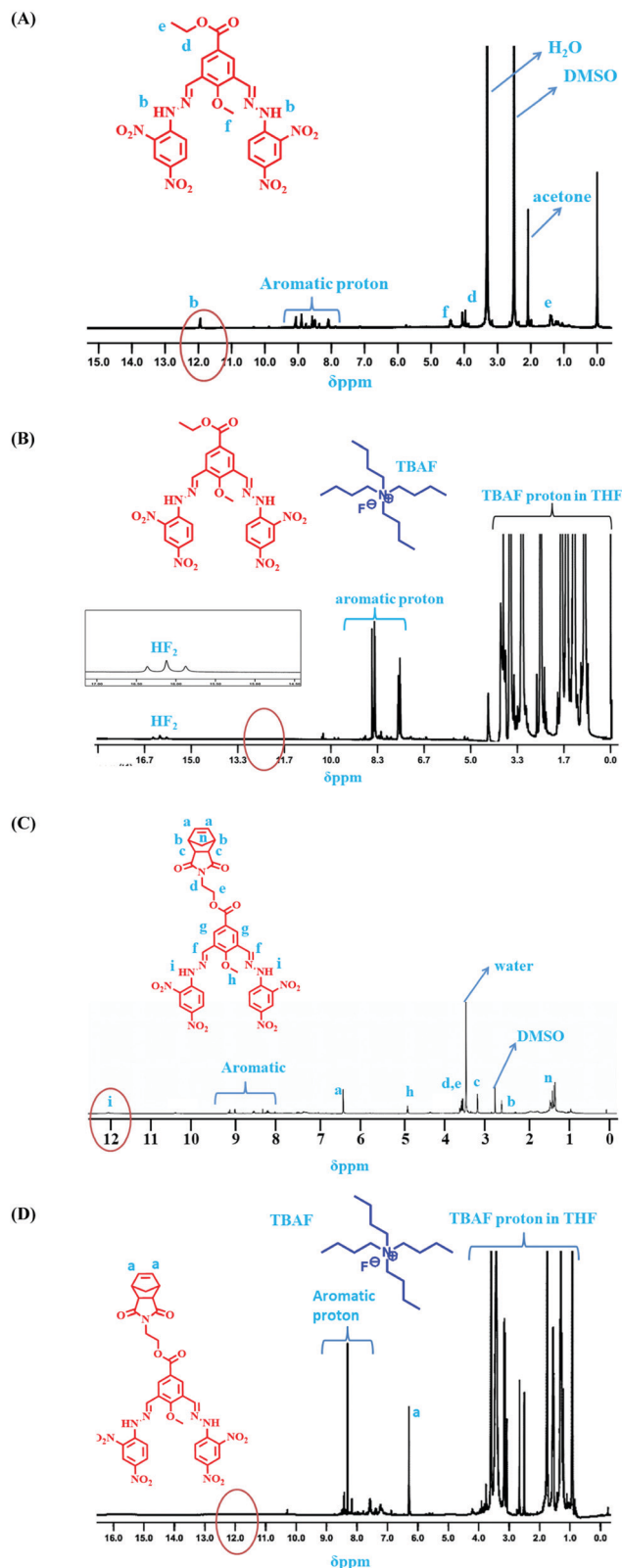
Fig. 6 ^{1}H NMR spectrum after the addition of TBAF (10^{-2} M) to (A) compound **4** (10^{-3} M); (B) after the addition of TBAF to compound **4** (10^{-3} M); (C) compound **9** (10^{-3} M); (D) after the addition of TBAF to compound **9** (10^{-3} M) in DMSO-d$_6$.
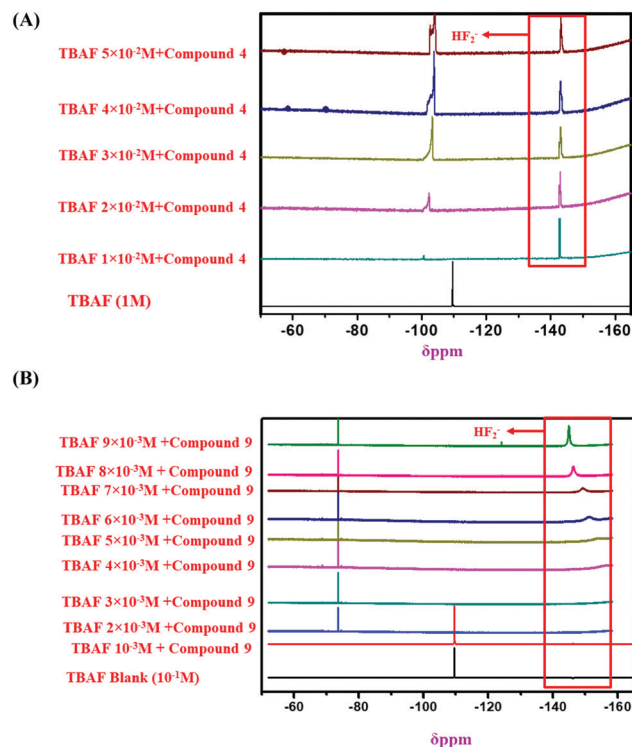

Fig. 7 ^{19}F NMR titration spectra of (A) compound **4** (10^{-2} M); (B) compound **9** (10^{-2} M) with the addition of TBAF (1 M and 10^{-1} M as the stock solution) in DMSO-d$_6$.
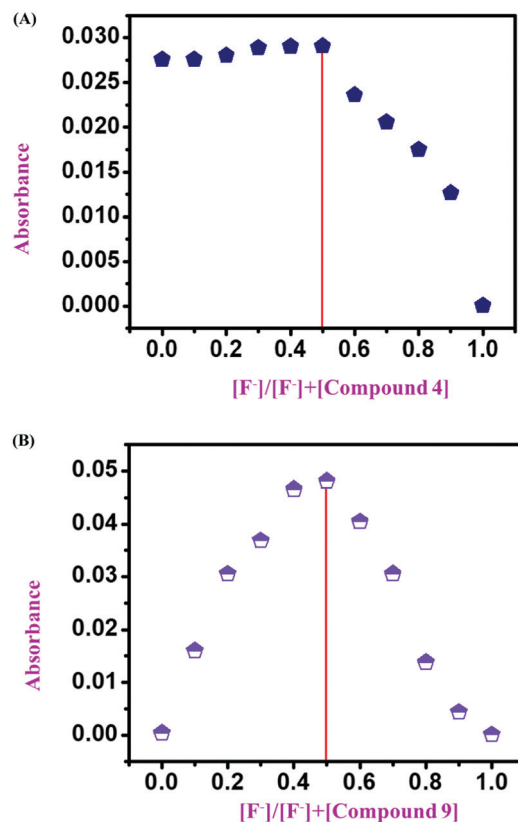

Fig. 8 Job's plot for (A) compound **4** and (B) compound **9**.

spectra were recorded after every addition of F^- ions, and all the ^{19}F NMR data were plotted. From the ^{19}F NMR titration plot, for compound **9, the** first peak appeared at -75 ppm; with the gradual addition of F^- ions, another peak appeared in the ^{19}F NMR spectra at -150 ppm. At a higher concentration of F^- ions, both peaks at -75 ppm and -150 ppm existed in the ^{19}F NMR spectra. This observation confirmed that sensor compound **9** first formed a complex with the analyte through a strong H-bonding interaction, which corresponded to the peak at -75 ppm, and then formed HF_2^- with the gradual addition of F^- ions by abstracting H from the sensor molecule, which corresponded to the other peak at -150 ppm. Based on all the ^{19}F NMR titration spectra, both monomeric sensors were found to result in a similar type of interaction (Fig. 7).

3.3 Job's plot

After confirmation of the sensing mechanism by UV-vis spectral analysis (both comparative and titration spectra), ^1H NMR titration, and ^{19}F NMR titration, we concluded the interaction mechanism for both monomeric sensors (compound **4** and compound **9**) concerning F^- ion concentration. For this, we considered both monomeric sensors' concentration (10^{-4} and 10^{-3} M as stock) and analyte concentration (TBAF 10^{-4} M). Then, a series of samples was used for UV-vis

spectral analysis by varying the mole fraction of both sensors and analyte in the range of 0 to 1. Then a UV-vis experiment was performed for every set of samples. After that, the UV-absorption data were plotted against the mole fraction of the F^- ion to obtain a Job's plot. It was observed that at the anion mole fraction of 0.5, the absorption value for the sensor molecule was maximum. This value confirms that the monomeric sensors (compound **4** and compound **9**) formed a 1:1 complex with the F^- ion (10^{-4} M and 10^{-3} M) (Fig. 8).
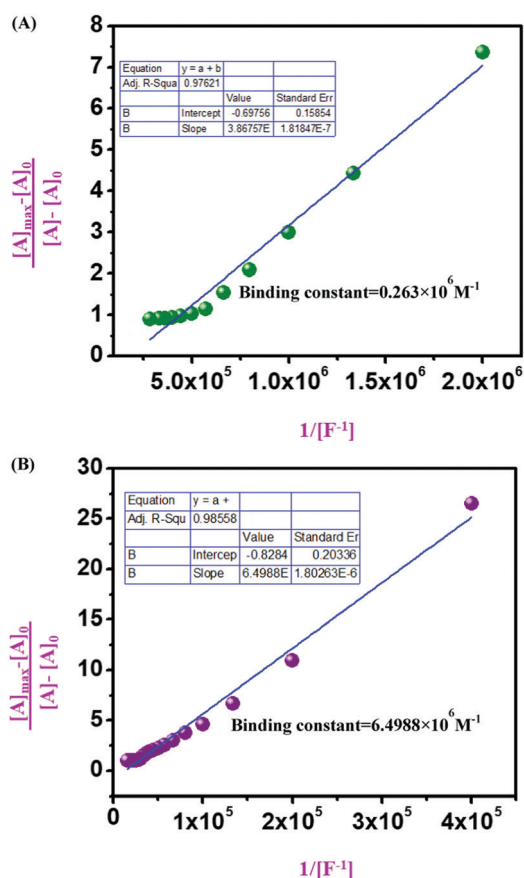

Fig. 9 Benesi–Hildebrand diagram plotting absorption at λ_{max} 537 nm for (A) compound **4**; (B) compound **9** (in DMSO : H_2O 9 : 1 v/v solution with Tris–HCl buffer at pH 7.4).
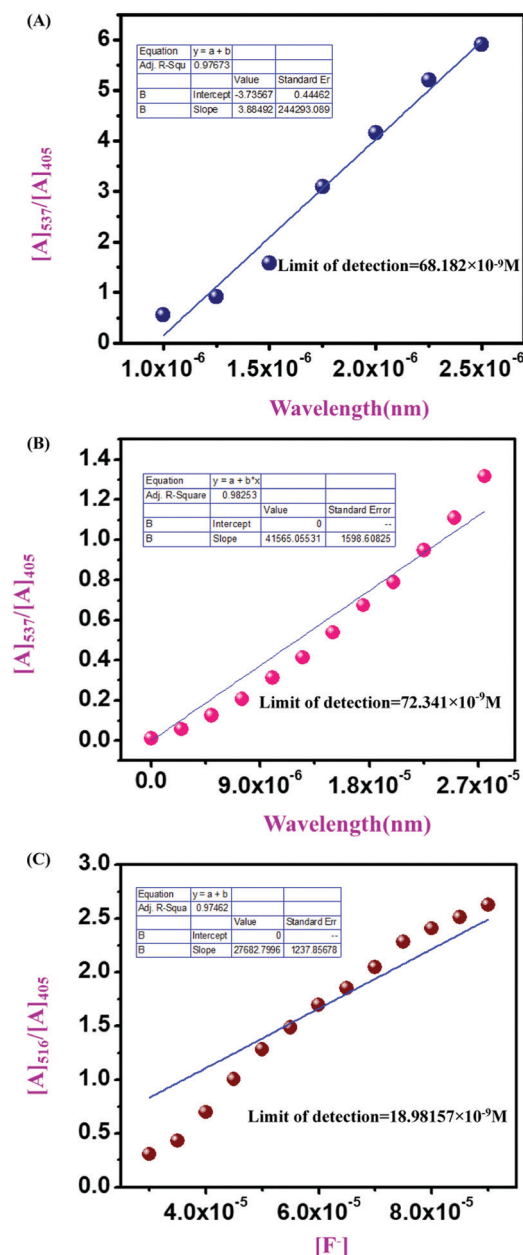

Fig. 10 Plots of A_{537}/A_{406} *versus* $[F^-]$ ranging from 1.0×10^{-6} M to 2.5×10^{-5} M for (A) (compound **4**); (B) compound **9** (in DMSO : H_2O 9 : 1, v/v solution with Tris–HCl buffer at pH 7.4). Plots of A_{516}/A_{405} *versus* $[F^-]$ ranging from 0 to 2.7×10^{-5} M and 8.0×10^{-5} M for (C) compound **11** (in DMSO : H_2O 9 : 1, v/v solution with Tris–HCl buffer at pH 7.4).

3.4 Binding constant and limit of detection (LOD)

From UV-vis spectroscopic concentration-dependent analysis for compound **4** (2.5×10^{-6} M) and compound **9** (1.5×10^{-5} M), it was observed that with the increase in F^- ion concentration, a ratiometric change occurred in the spectra. Absorbance maxima were shifted from λ_{max} 405 nm to λ_{max} 537 nm with the generation of an isosbestic point at λ_{max} 444 nm and a drastic naked eye color change occurred from light yellow to dark pink. From the titration between sensor and analyte, the binding constant or association constant of sensors with the analyte was calculated by using the Benesi–Hildebrand equation. For calculating the binding constant, we considered the absorbance value of monomeric sensors at λ_{max} 537 nm, which appeared with the gradual addition of F^- ions (10^{-4} M and 10^{-3} M TBAF stock solutions). A linear fitting plot was obtained by plotting $[A_{max}] - [A_0]/[A] - [A_0]$ *versus* $1/[F^-]$, and the reciprocal value of the slope of that linear fitted plot was the binding constant for both sensors towards F^- ions, where $[A]$ is the absorbance of the sensor molecule at λ_{max} 537 nm at a particular concentration of the F^- ion, $[A_0]$ is absorbance at λ_{max} 405 nm at that particular rF^- ion concentration, and $[A_{max}]$ is maximum absorbance at λ_{max} 537 nm among all absorbance values at λ_{max} 537 nm. From the Benesi–Hildebrand plot, the binding constant was 0.263×10^6 M^{-1} for compound **4** and 6.4988×10^6 M^{-1} for compound **9** (Fig. 9).

Furthermore, the corresponding absorbance *vs.* concentration of F^- ions for compound **4** (2.5×10^{-6} M) (Fig. 10A), compound **9** (1.5×10^{-5} M) (Fig. 10B), and compound **11** (1 mg/2 mL solvent) (Fig. 10C) has been used for calculating the LOD. The limit of detection has been calculated using LOD = $3\sigma/k$, where k is the slope of each linear plot for the mentioned sensors, and σ is the standard deviation of blank measurements. With this, the calculated LOD values for compound **4**, compound **9**, and compound **11** are 68.182×10^{-9} M, 72.341×10^{-9} M, and 18.98157×10^{-9} M, respectively.

4. Time-dependent analysis and real sample analysis

The response of the sensors towards F^- ions was within 3 minutes for compound **4** (Fig. S24, ESI†), compound **9** (Fig. S25, ESI†), and compound **11** (Fig. S26, ESI†) from the UV-vis experiment. For real sample analysis, a F^- ion-containing branded toothpaste was collected from a nearby supermarket. After that, 100 mg of that toothpaste was dissolved in 10 mL of HPLC grade water. Then the toothpaste solution was centrifuged for 30 min, and the residual solution was filtered down by syringe filtration. Then, a UV-vis spectroscopic analysis was performed using compounds **4**, **9**, and **11** with the toothpaste solution, respectively. For the analysis, compound **4** (2.5×10^{-6} M), compound **9** (1.5×10^{-5} M) and compound **11** were taken as 1 mg/2 mL DMSO : H$_2$O 9 : 1 v/v, in Tris–HCl buffer of pH 7.4. To the solution of both monomeric and polymeric sensors of 100 μL, a toothpaste solution was added, and UV-vis analysis was done. In the recovery experiments, the spiked samples were obtained by adding standard solutions with varying F^- ion concentrations into the toothpaste samples. The recovered F^- ion concentration obtained from analysis was 1.2×10^{-6} M using compound **4** (Fig. S27, ESI†), 1.016×10^{-6} M using compound **9** (Fig. S28, ESI†), and 0.9213×10^{-6} M using compound **11** (Fig. S29, ESI†).
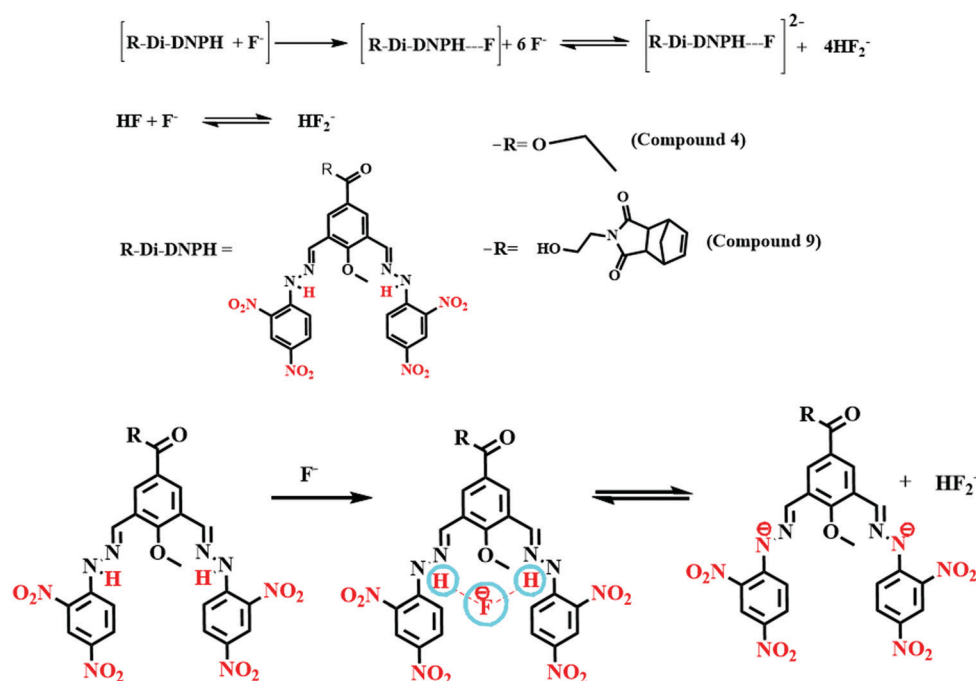

Fig. 11 Binding mechanism of fluoride and sensor compound **4** and compound **9**.

5. Mechanism of interaction of sensors with analyte

From all the above analytical studies, the interaction mechanism of all monomeric (compound **4** and compound **9**) and polymeric sensors (compound **11**) with F^- ions was confirmed. The Job's plot confirms the 1 : 1 binding stoichiometry of the monomeric sensors with F^- ions (Fig. 8). Then, ^1H NMR and ^{19}F NMR titrations confirmed the actual interaction mechanism (both strong H-bond formation and abstraction of H-atoms to produce HF_2^- species) of the sensors using the analyte (Fig. 6 and 7). As the F^- ion is smaller in size among all the halides, and negative charge density is also high, this makes F^- ions a hard base in nature. Due to that hard nature, it can abstract the H-atom (hard acid) from –NH groups of the sensors, simultaneously forming HF_2^- in the medium and generating negative charge on the molecules (all monomeric and polymeric sensors). This negative charge on all sensors acts as a donor site, and the electron-withdrawing $-NO_2$ group of the DNPH moiety acted as an acceptor site. Due to the presence of donor and acceptor sites in the same sensor molecule, a strong ICT (intermolecular charge transfer) occurred from the negatively charged dense donor site (NH– group) to the electron-withdrawing acceptor site (NO_2 group), which was confirmed by both ^1H NMR and ^{19}F NMR titration studies (Fig. 6 and 7).[39] Also, in the presence of two 2,4-DNPH groups, a nice cavity was produced by the sensor molecules for F^- ions only (as an acetate anion does not interfere with the F^- ion). So, it can be concluded that both the species ([sensors + F^- ion] and [sensors]$^{2-}$) were present in the solution for all the sensors (compound **4**, compound **9**, and compound **11**). The pictorial representation of the interaction mechanism for F^- ions with the sensors is given below in Fig. 11.

6. Conclusion

In conclusion, the sensors were synthesized successfully and well-characterized by ^1H NMR, ^{13}CNMR, HRMS, and FTIR spectroscopies. All these sensors show a selective colorimetric response (from light yellow to dark pink) at a micromolar level in semi-aqueous medium with F^- ions. The binding interaction with sensors was investigated by performing ^1H NMR, ^{19}F NMR, and UV-vis spectroscopic titrations. The analysis proved that the binding ratio was 1 : 1 (from the Job's plot) due to H-bonding interaction between the sensors and F^- ions. The drastic color change from yellow to pink was due to H-atom abstraction by the probe and ICT from the N–H group, with the high electron-withdrawing nitro groups. Hence, we have successfully explained all the syntheses, analyses of monomeric and polymeric sensors, and the mechanism of interaction of the analyte with the sensors.

Abbreviations

ICT Intermolecular charge transfer
2,4-DNPH 2,4-Dinitrophenyl hydrazine

Conflicts of interest

There are no conflicts to declare.

Acknowledgements

References

1 D. A. Jose, S. Mishra, A. Ghosh, A. Shrivastav, S. K. Mishra and A. Das, Colorimetric sensor for ATP in aqueous solution, *Org. Lett.*, 1979, **2007**, 10.

2 S. Saha, A. Ghosh, P. Mahato, P. Misra, S. K. Mishra, E. Suresh, S. Das and A. Das, Specific Recognition and Sensing of CN^- in Sodium Cyanide Solution, *Org. Lett.*, 2010, **15**, 34063.

3 D. Jose, D. K. Kumar, B. Ganguly and A. Das, Efficient and simple colorimetric fluoride ion sensor based on receptors having urea and thiourea binding sites, *Org. Lett.*, 2004, **20**, 3445.

4 A. Maity, F. Ali, H. Agarwal, B. Anothumakkoolb and A. Das, Tuning of multiple luminescence output and white-light emission from a single gelator molecule through an ESIPT coupled AIEE process, *Chem. Commun.*, 2015, **51**, 2130.

5 US EPA, National primary drinking water regulations, fluoride, final rule and the proposed rule, US Environmental protection Agency, Federal Register, 1985b, 50(220), 47142.

6 A. Salifu, B. Petrusevski, K. Ghebremichael, R. Baumah and G. Amy, Multivariate statistical analysis for fluoride occurrences in groundwater in the northern region of ghana, *J. Contam. Hydrol.*, 2012, **140–141**, 34–44.

7 Exposure to inadequate or excess fluoride: a major public health concern (WHO, 2019), https://apps.who.int/iris/bitstream/handle/10665/329484/WHO-CED-PHE-EPE-19.4.5-eng.pdf?ua=1.

8 K. Brindha and L. Elango, in Fluoride in Groundwater: Causes, Implication, and Mitigation Measures, *Fluoride Properties, Application and Environmental Management*, ed. S. D. Monroy, 2011, p. 111.

9 H. P. Petrone, M. Giordano, S. Giustino and M. F. Guarino, Enduring Fluoride Health Hazard for the Vesuvius area population: The Case ofAD 79 Herculaneum, Endemic Fluorosis at Vesuvius, *PLoS One*, 2011, **6**, 1.

10 P. Das, M. K. Kesharwani, A. K. Mandal, E. Suresh, B. Ganguly and A. das, An alternative approach: a highly selective dual responding fluoride sensor having active methylene group as a binding site, *Org. Biomol. Chem.*, 2012, **10**, 2263.

11 S. Roy, A. Maity, N. Mudi, M. Shyamal and A. Mishra, Rhodamine scaffolds as real-time chemosensors for selective detection of bisulfite in an aqueous medium, *Photochem. Photobiol. Sci.*, 2019, **18**, 1342.

12 Y. Jo, N. Chidalla and D. Cho, Bis-ureidoquinoline as a Selective Fluoride Anion Sensor through Hydrogen-Bond Interaction, *J. Org. Chem.*, 2014, **79**, 9418.

13 D. E. Gomez, L. Fabbrizzi and M. Licchelli, Why, on Inter-action of Urea-Based Receptors with Fluoride, Beautiful Colors Develop, *J. Org. Chem.*, 2005, **70**, 5717.

14 M. Shyamal, P. Mazumdar, S. Maity, S. Samanta, G. P. Sahoo and A. Misra, Highly Selective Turn-On Fluorogenic Chemo-sensor for Robust Quantification of Zn(2) Based on Aggre-gation Induced Emission Enhancement Feature, *ACS Sens.*, 2016, **6**, 739.

15 X. Cao, W. Lin, Q. Yu and J. Wang, Ratiometric sensing of fluoride anions based on a BODIPY-coumarin platform, *Org. Lett.*, 2011, **22**, 6098.

16 S. Sarkar and R. Shunmugam, Unusual redshift of the sensor while detecting the presence of Cd^{2+} in the aqueous environment, *ACS Appl. Mater. Interfaces*, 2013, **5**, 7379.

17 I. S. Turan and E. U. Akkaya, Chemiluminescence Sensing of Fluoride Ions Using a Self-Immolative Amplifier, *Org. Lett.*, 2014, **16**, 1680.

18 P. Thiampanya, N. Muangsin and B. Pulpoka, Azocalix[4]arene Strapped Calix[4]pyrrole: A Confirmable Fluoride Sensor, *Org. Lett.*, 2012, **14**, 4050.

19 M. Thakeuchi, T. Shioya and T. M. Swager, Allosteric Fluoride Anion Recognition by a Doubly Strapped Porphyrin, *Angew. Chem., Int. Ed.*, 2001, **40**, 3372.

20 J. M. Stauber, G. E. Alliger, D. G. Nocera and C. C. Cummins, Second-Coordination-Sphere Assisted Selective Colori-metric Turn-on Fluoride Sensing by a Mono-Metallic Co(II) Hexacarboxamide Cryptand Complex, *Inorg. Chem.*, 2017, **56**, 7615.

21 H. Aboubakr, H. Brisset, O. Siri and J. Raimundo, Highly Specific and Reversible Fluoride Sensor Based on an Organic Semiconductor, *Anal. Chem.*, 2013, **85**, 9968.

22 A. S. Oshchepkov, T. A. Shumilova, S. R. Namashivaya, O. A. Fedorova, P. V. Dorovatovskii, V. N. Khrustalev and E. A. Kataev, Hybride Macrocycles for Selective Binding and Sensing of Fluoride in Aqueous Solution, *J. Org. Chem.*, 2018, **83**, 2145.

23 P. A. Gale and C. Caltagirone, Anion sensing by small molecules and molecular ensemble, *Chem. Soc. Rev.*, 2015, **44**, 4212.

24 R. Kaushik, R. Sakla, A. Ghosh, G.t. Selvan, P. M. Selvakumar and D. A. Jose, Selective Detection of H_2S by Copper Complex Embedded in Vesicles Through Metal Indicator Displacement Approach, *ACS Sens.*, 2018, **3**, 1142.

25 R. Shunmugam, G. J. Gabriel, C. E. Smith, K. A. Aamer and G. N. Tew, A Highly Selective Colorimetric Aqueous Sensor for Mercury, *Chem. – Eur. J.*, 2008, **14**, 3904.

26 S. Bhattacharya, S. Sarkar and R. Shunmugam, Unique norbornene polymer-based "in-field" sensor for As(III), *J. Mater. Chem. A*, 2013, **1**, 8398.

27 S. D. Starner, S. Arungundram and C. H. Saunders, Anion sensors based on b,b′-disubstituted porphyrin derivatives, *Tetrahedron Lett.*, 2002, **43**, 7785.

28 R. Sivakumar, V. Reena, N. Anathi, M. Babu, S. Anandan and S. Velmathi, Colorimetric and fluorescence sensing of fluoride anion with potential salisaldimine based Schiff base receptor, *Spectrochim. Acta, Part A*, 2010, **75**, 1146.

29 A. Sahana, A. Banerjee, S. Lohar, S. Panja, S. K. Mukhopadhyay, J. S. Matalobos and D. Das, Fluorescence sensing of arsenate at a nanomolar level in a greener way: a naphthalene-based probe for living cell imaging, *Chem. Commun.*, 2013, **49**, 7231.

30 J. F. Lamere, N. Saffon, I. D. Santos and S. F. Forgues, Aggregation-induced emission enhancement in organic ion pairs, *Langmuir*, 2010, **26**, 10210.

31 G. J. Mao, T. T. Wei, X. X. Wang, S. Y. Huan, D. Q. Lu, J. Zhang, X. B. Zhang, W. H. Tan, G. I. Shen and R. Q. Yu, High-Sensitivity Naphthalene-Based Two-Photon Fluores-cent Probe Suitable for Direct Bioimaging of H_2S in Living Cells, *Anal. Chem.*, 2013, **85**, 7875.

32 Y. Zhou, J. F. Zhang and J. Yoon, Fluorescence and colori-metric chemosensors for fluoride-ion detection, *Chem. Rev.*, 2014, **114**, 5511.

33 K. B. Wiberg and D. J. Rush, Solvent Effect on the Thio-amide Rotational Barrier: An Experimental and Theoretical Study, *J. Am. Chem. Soc.*, 2001, **123**, 2038.

34 E. W. Seo, J. H. Han, C. H. Heo, J. H. Shin, H. M. Kim and B. R. Chao, A Small-Molecule Two-Photon Probe for Nitric Oxide in Living Tissues, *Chem. – Eur. J.*, 2012, **18**, 12388.

35 Z. Dai, L. Tian, B. Song, X. L. Lui and J. L. Yuan, Develop-ment of a novel lysosome-targetable time-gated luminescence probe for ratiometric and luminescence lifetime detection of nitric oxide in vivo, *Chem. Sci.*, 2017, **8**, 1969.

36 C. G. Dai, J. L. Wang, Y. L. Fu, H. P. Zhou and Q. H. Song, Selective and Real-Time Detection of Nitric Oxide by a Two-Photon Fluorescent Probe in Live Cells and Tissue Slices, *Anal. Chem.*, 2017, **89**, 10511.

37 D. A. Jose, P. Kar, D. Koley, B. Ganguly, W. Thiel, H. N. Ghosh and A. Das, Fluoride Ion Receptor Based on Dipyrrolyl Derivatives Bearing Electron-Withdrawing Groups: Synthesis, Optical, and Electrochemical Sensing and Computational Studies, *Inorg. Chem.*, 2007, **46**, 5576.

38 R. Pegu, R. Mandal, A. K. Guhab and S. Pratihar, A selective ratiometric fluoride ion sensor with a (2,4-dinitrophenyl) hydrazine derivative of bis(indolyl) methane and its mode of interaction, *New J. Chem.*, 2015, **39**, 5984.

39 L. K. Kumawat, A. A. Abogunrin, M. Kickham, J. Pardeshi, O. Fenelon, M. Schroeder and R. B. P. Elmes, Squaramide-Napthalimide Conjugates as 'Turn-On' Fluorescent Sensors for Bromide Through an Aggregation-Disaggregation Approach, *Front. Chem.*, 2019, **7**, 354.

40 A. Aydogan, A. Koca, M. K. Sener and J. L. Sessler, EDOT-functionalized calix [4] pyrrole for the electrochemical sensing of fluoride in water, *Org. Lett.*, 2014, **16**, 3764.

41 D. A. Jose, D. K. Kumar, B. Ganguly and A. Das, Efficient and simple colorimetric fluoride ion sensor based on receptor having urea and thiourea binding sites, *Org. Lett.*, 2004, **6**, 3445.

42 H. Tong, L. Wang, X. Jing and F. Wang, ''TURN-ON'' conjugated polymer fluorescent chemosensor for fluoride ion, *Macromolecules*, 2003, **36**, 2584.

43 H. A. Benesi and J. H. Hilderbrand, A Spectrophotometric Investigation of the Interaction of Iodine with Aromatic Hydrocarbon, *J. Am. Chem. Soc.*, 1949, **71**, 2703.

44 D. Sharma, S. K. Sahoo, S. Chaudhary, R. K. Bera and J. F. Challan, Fluorescence 'turn-on' sensor for F^- derivative from vitamin B_6 cofactor, *Analyst*, 2013, **138**, 3646.

45 S. K. Sahoo, G. D. Kimb and H. G. Choi, Optical sensing of anions using C_{3v}-symmetric tripodal receptors, *J. Photochem. Photobiol., C*, 2016, **27**, 30–53.